GEOLOGICA CARPATHICA, 2024, 75, 6, 359–374 https://doi.org/10.31577/GeolCarp.2024.22

The geochemical character of synsedimentary volcanism in the Permian Haselgebirge Formation of the Eastern Alps (Austria): Implications for paleogeographic models

CHRISTOPH LEITNER[1,✉], CHRISTOPH A. HAUZENBERGER[2], H. ALBERT GILG[3], GERTRUDE FRIEDL[1], CHRISTOPH VON HAGKE[1] and FRIEDRICH FINGER[4]

[1]University of Salzburg, Fachbereich Umwelt & Biodiversität, Hellbrunner Straße 34, 5020 Salzburg, Austria
[2]University of Graz, Institut für Erdwissenschaften, Universitätsplatz 2, 8010 Graz, Austria
[3]Technical University of Munich, Lehrstuhl für Ingenieurgeologie, Arcisstraße 21, 80333 München, Germany
[4]University of Salzburg, Fachbereich Chemie und Physik der Materialien, Jakob-Haringer-Strasse 2a, 5020 Salzburg, Austria

(Manuscript received August 12, 2024; accepted in revised form January 21, 2025; Associate Editor: Igor Broska)

Abstract: We investigated the geochemistry of ca. 50 volcanic rock samples collected in various regions of the ca. 250 Ma old evaporite-bearing Austroalpine Haselgebirge Formation. The rocks are interpreted to represent synsedimentary volcanism in the Haselgebirge Formation. Open system low-T alteration processes have severely altered potassium, sodium, and calcium contents. However, based on immobile trace elements such as Zr, Y, Nb, Ti, the Haselgebirge volcanism can be classified as mainly basaltic. Different mantle sources must have been at play. Volcanism in the eastern part of the Haselgebirge Formation (Annaberg, Pfennigwiese) was MORB-like and probably related to asthenospheric mantle upwelling. As opposed to this, the volcanic samples of the western Haselgebirge Formation (Hallstatt, Lammertal) display predominantly alkali-basaltic trace element characteristics. It is hypothesized that they represent magmas from a metasomatized lithospheric mantle. Finally, a third basalt type with remarkably low Nb and Ta contents could be identified in the locality Wienern. It might be related to a (remnant?) subduction-modified mantle source. Our research highlights a gradual change of the type of magmatic activity in the Austroalpine Unit during the Permian. While according to literature data, magmatism in the early and middle Permian was dominantly felsic (granitic) and crustal, mafic mantle magmatism apparently gained increasing importance by the end of the Permian. This likely mirrors the beginning break-up of the local Pangea crust and the upwelling of asthenospheric mantle antedating the Triassic opening of the Meliata ocean. The observed source variations within the Haselgebirge volcanism point to a comparably greater degree of lithosphere thinning in the east. This accords with geological models where the (Triassic) Meliata ocean gained its greatest width in the Carpathian realm while wedging out towards the western Eastern Alps.

Keywords: Northern Calcareous Alps, Haselgebirge Formation, volcanites, geochemistry, immobile trace elements

Introduction

Magmatism typically accompanies the break-up of a continent, but the produced magma types can be significantly different (Wilson 1989; Schmincke 2012). Unresolved questions center around the nature of the involved mantle sources and, in particular, the role of mantle metasomatism through melts or fluids (e.g., Pilet et al. 2011; Rowe et al. 2015; Xia & Li 2019; White et al. 2020; Tortelli et al. 2022; Binder et al. 2024). A prominent example of a continental break-up situation with magmatic activity can be studied in the Permotriassic of the Eastern Alps. Permian rocks in this region witness a period of crustal extension, which resulted subsequently in the formation of Triassic ocean floor inboard of Pangea (Meliata ocean). According to the paleogeographic model of Stampfli (1996), Stampfli & Mosar (1999), and Stampfli et al. (2013) the Meliata ocean formed as a small ribbon in the back-arc realm of the Paleotethys subduction zone. An alternative paleogeographic scenario is advocated by Haas et al. (1995) and Schmid et al. (2008). Here, the Meliata oceanic realm is interpreted as the northernmost tip of the large Neotethys oceanic rift, which opened between Greater Adria and Dacia/Cimmeria (van Hinsbergen et al. 2020).

Traces of Meliata ocean floor are mainly preserved in the West Carpathians (Horváth 2000; Putiš et al. 2023) but also in the Austroalpine unit in the form of rare Triassic metabasite, ultrabasite and radiolarite rocks (Kozur 1991; Mandl & Ondrejičková 1991; Gawlick & Missoni 2015; Strauss et al. 2023 and references therein). Relics of Permian ophiolites have not yet been encountered in the Eastern Alps. However, a famous occurrence of a Permian metagabbroic rock in the Koralpe (now eclogite) with a MORB-like geochemical signature (Thöni 2006; Miller et al. 2007; Chang et al. 2023) has tentatively been interpreted to herald the opening of the Meliata ocean. Speculations about incipient ocean floor spreading in the latest Permian received further support

✉ corresponding author: Christoph.Leitner
Christoph.Leitner@plus.ac.at

through local studies of synsedimentary volcanites in the (ca. 250 Ma old) Haselgebirge Formation, which revealed a presence of MORB-type pillow basalts (Kirchner 1979, 1980; Kralik et al. 1984; Gruber et al. 1992). As opposed to this, Schorn et al. (2013) presented geochemical analyses of other Haselgebirge volcanic rocks from the location Moosegg (Lammertal), which indicated within-plate-basalt.

In an attempt to better assess the apparently complicated overall situation and in order to expand our knowledge regarding the Permian magmatism in the Eastern Alps and its tectonic environment, we present and discuss here a new large set of geochemical data for volcanic rock fragments sampled systematically all over the late Permian Haselgebirge Formation. Because of the generally strong alteration of most of these samples, our inferences on magma characteristics are preferentially based on discrimination diagrams that use immobile trace elements like Zr, Y, Nb, Ti (e.g., Winchester & Floyd 1977; Pearce & Norry 1979; Pearce 1983).

Geological background

Permian graben tectonics is a prominent feature all over Europe, unequivocally indicating a period of large-scale crustal extension in that part of the Pangea continent (Ziegler 1990; Meier et al. 2016; Mouthereau et al. 2021). The grabens strike E–W in today coordinates. The extensional stresses were possibly related to a large-scale reorganization of the Pangean plate kinematics at the end of the Variscan orogeny. While major Variscan subduction systems became abandoned, new subduction zones came into being in other places (Nikishin et al. 2002). This has likely changed the mantle convection system underneath the proto-European Pangea sector. Increased mantle heat flow led to a thermal erosion of the mantle lithosphere and to a new isostatic equilibrium (Ziegler 1990, 1993; Nikishin et al. 2002; Ziegler & Dèzes 2006; Meier et al. 2016; Mouthereau et al. 2021). In addition, given that a Permian Paleotethys subduction system existed (Stampfli et al. 2013), processes of back-arc extension could have been significant in the proto-Alpine part of Pangea (Meier et al. 2016). In the early Triassic, the Dacia/Cimmerian land split from Greater Adria and the Neotethys was opened. According to van Hinsbergen et al. (2020) the Neotethys rift was N–S oriented in present day coordinates.

Considering the Alps, Permian grabens are known from underneath the Molasse Zone (McCann et al. 2006), the Western (Pfiffner 2014) and Eastern Alps (Krainer 1993; Veselá & Lammerer 2008; Veselá et al. 2008) as well as the Southern Alps (Sciunnach 2003; Berra & Felletti 2011). The extensional environment persisted from ca. 290 to 250 Ma (Schuster et al. 2001; Schuster & Stüwe 2008). The Permian sedimentary record in the Alps comprises mainly sandstones and conglomerates known as "Verrucano", Lantschfeld Formation, Fellersbach Formation, etc. (Tollmann 1963, 1985; Neubauer 1988; Krainer 1993; Hubmann et al. 2014). It has been reported that these rocks contain abundant detritus from Permian rhyolites (Faupl 1970; Tollmann 1972; Oberhauser 1980). Notably, some of the Permian clastic sediments lie transgressively over exhumed Variscan metamorphic rocks or granites, which demonstrates an ongoing exhumation process (Nievoll 1984; Reiser et al. 2024).

The Upper Austroalpine evaporitic Haselgebirge Formation was deposited during the latest Permian and contains accumulated halite, mudstone, sulfate rocks (gypsum/anhydrite) and dolomite (Spötl 1989). Evaporites of this type are found in many places throughout almost the entire Northern Calcareous Alps (Granado et al. 2019; Strauss et al. 2021) and in the Western Carpathians as well (Oravecz et al. 2023 and references therein). These rheologically weak Haselgebirge rocks rose later as diapirs into their thick Triassic carbonate cover and served as major detachment and glide level during Alpine nappe stacking (Neubauer & Genser 1990; Missoni & Gawlick 2011; Leitner & Spötl 2017; Ortner & Sinah 2022; Fernandez et al. 2024).

The paleogeographic positions of the Upper Permian Haselgebirge Formation and the associated Triassic Hallstatt facies formations were repeatedly discussed in the past (see e.g., Tollmann 1985). Kozur (1991) was the first who proposed a connection with the Carpathian basalt-bearing mélange of the Meliata unit. Two main types of paleogeographic models developed over time regarding the Meliata ocean: (1) The model of Stampfli (Stampfli 1996; Spahić 2024) views the Meliata ocean as a back-arc ocean of the Paleotethys. In this model, the Meliata ocean is independent and was never connected to the Neotethys ocean. (2) In the model of Haas et al. (1995), which relies mainly on facies aspects, the Meliata ocean is seen as part (the most northern branch) of the Neotethys (Schmid et al. 2008; Strauss et al. 2023). The Haselgebirge and Hallstatt facies formations are interpreted as part of a distal shelf towards the open Neotethyan ocean (e.g., Gawlick & Missoni 2015). Both models are discussed controversially until present, for review see Slovenec & Šegvić (2024).

Basement rocks exhumed during the Cretaceous–Paleogene Alpine tectonism provide important insight into the thermal evolution of the middle and lower Austroalpine crust during the Permian. They document widespread Permian metamorphism with an age of about 270 Ma (Thöni & Jagoutz 1993; Schuster et al. 2001; Thöni 2006; Miller et al. 2007; Schuster & Stüwe 2008). This Permian metamorphism in the Alps displays a high thermal gradient, with LP/HT metamorphic rocks of that age being known, for instance, from the Silvretta, Koralpe, Ivrea, Southern Alps and from south of the Tauern Window (Schuster et al. 2001; Petri et al. 2017). In addition, more and more Permian granitoid rocks are recognized in the Eastern Alps (Schulz 2017; Yuan et al. 2020; Neubauer et al. 2022; Putiš et al. 2024; Reiser et al. 2024). Most of these are early to mid Permian intrusions. Coeval felsic volcanic analogues are documented in both the Eastern and Southern Alps (Willcock et al. 2013). Minor felsic igneous activity is also documented in the late Permian/early Triassic (Habler et al. 2007; Miller et al. 2011; Chang et al. 2020; Knoll et al. 2023).

As highlighted in the introduction section, mafic intrusions and metabasalts of Permian age (later metamorphosed to eclogite in part) occur in the Saualpe/Koralpe/Pohorje mountains. According to new geochronological data in Chang et al. (2023) this magmatism lasted from ca. 280 to 240 Ma. Geochemically, these mafic rocks resemble mostly normal mid-ocean ridge basalts (Miller et al. 1988, 2007; Thöni & Jagoutz 1993; Miller & Thöni 1997; Sassi et al. 2004; Chang et al. 2023), however, an early Triassic gabbroic body at Eisenkappel shows a within-plate signature (Miller et al. 2011).

Methods

Sample locations

The Haselgebirge-bound volcanic rocks considered in this study are from four regions and locations, respectively. These are from west to east: the Lammertal (Lammer valley), the salt mine Hallstatt, the quarry of Wienern near Grundlsee, and the locations Annaberg and Pfennigwiese (Fig. 1). The presence of volcanic rock relics in these sites is long known from the literature (see below). However, while the previous studies on these rocks were mainly local and with a mineralogical emphasis, we attempt here for the first time to draw a complete geochemical picture for the Haselgebirge volcanism based on a systematic sampling campaign over the whole Northern Calcareous Alps. From all known occurrences of volcanic rocks only one in the salt mine Bad Ischl (Vozárová et al. 1999) remained unconsidered in our study, because suitable sample material could not be procured.

Our sample set includes compact, subangular volcanic boulders of centimeter to decimeter size collected in the neighborhood of evaporite rocks such as halite, anhydrite, or remnants of evaporite-bearing rocks, i.e. gypsum, rauhwacke and weathered mudstone, respectively. Even though direct contacts to these Haselgebirge sediments are only rarely observable, we argue for a mainly synsedimentary late Permian (ca. 250 Ma) age of the volcanic rock fragments. See discussion for arguments.

The *Lammertal* (Lammer valley; Fig. 1) provides a large exposure of deeply weathered Haselgebirge mudstone (Plöchinger et al. 1982). Volcanic inlayers were described by Kirchner (1979, 1980). On revisiting the area, we found and took 16 volcanic rock samples from the location Webing, and from two places along the creek Rigausbach. Volcanic rocks from the *salt mine of Hallstatt* have been described by von Hauer (1879) and Zirkl (1957) with a particular reference to their generally severe mineralogical alteration phenomena. A syngenetic contact between basalt and mudstone in the mine was studied by Leitner et al. (2017) and interpreted in terms of a subaerial deposition of the lava flow and later submergence. Leitner et al. (2017) have also published 6 geochemical analyses for this ca. 30 m thick basalt layer, which are included in the present paper. From the gypsum mine of *Wienern* Kirchner (1979) reported thinly bedded tuffs and tuffites as well as more massive metabasalts with pillow structures. The latter imply a subaquatic depositional environment. We collected 11 volcanic samples from this quarry. The volcanic rocks of the locations *Annaberg* and *Pfennigwiese* occur together with sulfate evaporites (Summesberger 1991). Kralik et al. (1984) and Gruber et al. (1992) have described them as strongly altered, partly spilitized oceanic tholeiite basalts. We collected samples at the locations Annaberg (8 samples) and Pfennigwiese (7 samples).

Laboratory methods

Samples were analysed for major and many trace elements using routine X-ray fluorescence (XRF). Analyses were carried out on a wave-length dispersive XRF spectrometer Bruker S4 explorer at the Department of Chemistry and Physics of Materials, University of Salzburg, equipped with a 4 kW Rh-anode tube. Major elements were determined on glass beads at reduced tube energies. Relative 2σ uncertainties were

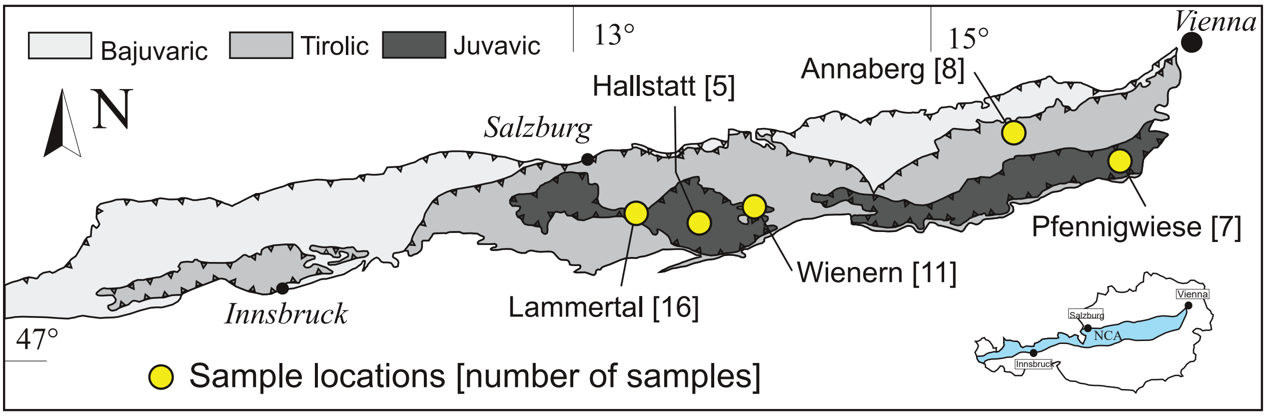

Fig. 1. Map showing the sampled volcanite-bearing Haselgebirge Formation occurrences in the Northern Calcareous Alps (NCA) of Austria. Nappe subdivision of the NCA is based on Oberhauser (1980).

better than 1 % for SiO_2 and Al_2O_3, and better than 5 % for elements at the 1–10 wt.% concentration level. For trace elements, which were measured on pressed powder pellets, counting times and tube conditions were optimized automatically up to 4 kW and 400 seconds per element, respectively, to obtain a detection limit of 3 ppm or better (3σ). Typical errors (2σ) from the counting statistics were 1–2 ppm at low concentrations (<10 ppm), 2–5 ppm at the 10–100 ppm concentration level, and better than 5 % (relative) for the rest.

Ten of the samples were additionally analysed by ICP-MS methods at the University of Graz. Approximately 40 mg sample powder were dissolved in a mixture of 1 ml double distilled HNO_3 (15 N) and 2 ml suprapure HF (28 N) in closed Teflon beakers on a hot plate at 200 °C for 48 h. This was followed by evaporation and consecutive re-dissolution in 1 ml HNO_3 (14 N) and 1 ml HCL (12 N). The sample was taken up with 2 % (v/v) HNO_3 to achieve a ~1500× dilution for analysis with an Agilent 7700 quadrupole ICP-MS at the Institute of Chemistry, University of Graz. Standards BHVO-2 (USGS) and IV-ICPM-71A (Inorganic Venture) were used for calibration and the additional standards JR-2, BCR-2, GS-N, MRH1 and MTA-1 were used for monitoring of accuracy. The detection limit was ca. 0.01 µg/g.

Thin sections were prepared for 14 samples and bulk powder mounts of these samples were investigated by X-ray powder diffraction (XRPD) analysis using a Bruker D8 Advance Eco diffractometer at Technical University of Munich (Cu K alpha, 40 kV, 25 mA, 2–75° 2 Theta, 0.01° 2Theta step size, 15 mm irradiated length, 2.5° primary and secondary sollers, and a Lynxeye XE-T detector). The mineral phases were identified on characteristic diffraction peaks and quantified using the Rietveld-program BGMN and the Profex graphical user interface (Bergmann et al. 1998; Döbelin & Kleeberg 2015). The phases in the selected thin sections have been identified by micro-Raman spectroscopy using a Horiba-Jobin-Yvon XploRA Plus device equipped with a frequency doubled Nd:YAG laser (532 nm, with a maximum power of 22.5 mW) and a Olympus LMPLFN 10× long distance objective with an aperture of 0.9.

Results

Petrography

A generally green colour testifies pervasive alteration of the volcanic rocks. However, a remnant volcanic (porphyric) fabric with white and/or dark euhedral pseudomorphs of former 1–5 mm sized magmatic phenocrysts is preserved in practically all sampled specimen (Fig. 2). White pseudomorphs, in thin section resolvable as aggregates of fine-grained albite (albitization), muscovite (sericitization), partly also secondary microcrystalline K-feldspar (potassium metasomatism), are interpreted as reaction products replacing magmatic plagioclase phenocrysts. Dark euhedral pseudomorphs, filled mainly with chlorite, likely represent former pyroxene crystals. Carbonatization, i.e., replacement of minerals through calcite, and associated formation of calcite veins, plays a role in some samples (e.g., PFE-1J), but is generally a less important alteration type in the volcanic rocks of the Haselgebirge.

Schlieren and a distinct alignment of the pseudomorphs probably feature lava flow structures. Amygdules are preserved in many samples as well. They are filled with quartz and subordinate calcite; in one case a galena filling was observed. Dark veinlets hosting quartz, carbonate, chlorite, and ore minerals indicate a certain hydrothermal element mobility. Another type of veins is filled with calcite. These veins form diffuse arrays of short length and occur predominantly in the anhydrite/gypsum deposits of Wienern and Pfennigwiese.

Despite of the preserved porphyritic and partly even ophitic textures, a substantial rock alteration is indicated in XRPD data showing a high degree of chloritization, albitization, and, in particular in the Lammertal samples, sericitization and secondary K-feldspar formation (Table 1). Only exceptionally clinopyroxene or primary plagioclase could be identified by XRPD and Raman spectroscopy.

Geochemistry

The chemical data for the sampled volcanic rocks are provided in Figs. 3–5 and Tables 2–5. As was expectable from the severe mineralogical alterations (see above), the rocks experienced postmagmatic chemical changes as well. Massive K-metasomatism is obvious in the Lammertal and Wienern volcanic samples, where K_2O whole rock contents are sometimes as high as 5–10 wt.%. The gain of K_2O is commonly coupled with a severe loss of Na_2O and CaO (Tables 3, 4). Interestingly, this K_2O metasomatism is much less developed in the samples of Annaberg and Pfennigwiese, which typically show K_2O contents around 1–2 wt.% (Table 2).

Carbonatization may have occasionally led to a certain gain (or regain) of CaO. Some samples show a high content of sulphur (e.g., WIE-32), which was obviously introduced from the surrounding Haselgebirge sediments.

The ratios of immobile trace elements Ti, Nb, Zr, Y and the diagram of Winchester & Floyd (1977) were used to infer primary rock compositions (Fig. 3). Based on this diagram, the investigated rocks are basaltic, but bimodal in the sense that they comprise alkali-basaltic endmembers as well as tholeiitic basalts to basaltic andesites.

There is a very remarkable regional trend: In the Lammertal region the volcanism is predominantly alkali-basaltic (only two samples from this area, LAM-4A and LAM-4I, plot as non-alkaline basalts/basaltic andesites). The data from the Hallstatt mine (Leitner et al. 2017) also point to alkali-basaltic volcanism, although the Nb/Y ratios are somewhat lower than in the neighbouring Lammertal region. In the eastern locations, Annaberg and Pfennigwiese, on the other hand, the volcanism was overwhelmingly tholeiitic (Fig. 3). Also, the sampled volcanic rocks from Wienern mostly classify as non-alkaline basalts/basaltic andesites in the Zr/Ti vs. Nb/Y diagram with

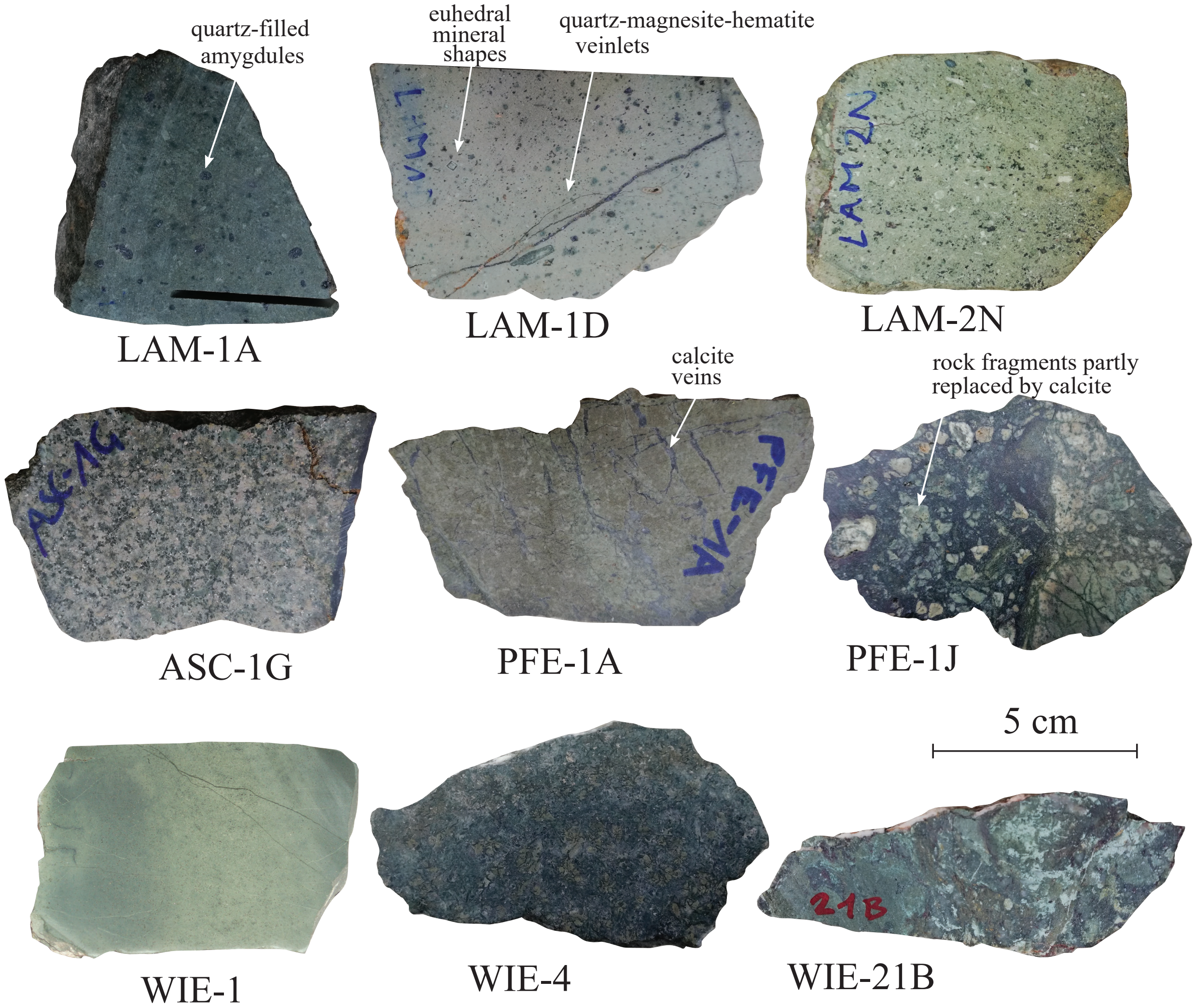

Fig. 2. A selection of the sampled and analyzed volcanic rocks. All rocks are strongly altered by chloritization (chlorite+quartz), sericitization, secondary K-feldspar, albitization, and carbonatization. LAM-1A is a typical porphyric volcanite with amygdules filled with quartz, LAM-1D shows quartz–magnesite–hematite veinlets, LAM-2N is a greenish porphyric volcanite with white inclusions (shapes of feldspar laths) and dark inclusions (shapes of pyroxen?), ASC-1G displays a bright matrix (albite and calcite after plagioclase) and numerous dark inclusions, PFE-1A is a fine-grained volcanite with chlorite-calcite veins, PFE-1J is a pyroclastic rock, the rock fragments are partly substituted by calcite, WIE-1 contains small needle-shaped inclusions, WIE-4 shows a poikilitic texture, laths and brown patches, WIE-21B is a strongly altered brecciated rock with macroscopically brownish-greenish-whitish patches, calcite patches and veins.

two samples plotting marginally in the andesite field. Only one sample from Wienern WIE-19 plots as alkali-basalt.

Interestingly, even in the most strongly K-metasomatized samples, the silica contents remain in the normal basaltic range. Likewise, Fe and Mg contents are in the normal basaltic range. It thus appears that Si, Fe and Mg behaved relatively immobile, as opposed to the alkali elements and the calcium. In one sample from the quarry Wienern (sample WIE 3) an exorbitantly high MgO content of 40 wt.% was measured in combination with high Cr (3597 ppm) and low Al_2O_3 (3 wt.%). We interpret this sample as an ultramafic rock.

Looking into a greater geochemically detail, the tholeiitic and alkali-basaltic magmatism in the Haselgebirge formation can be described as follows:

The ***alkali-basaltic*** samples are within-plate basalts according to the discrimination diagrams (Fig. 4) of Pearce & Norry (1979) and Pearce (1982). In MORB-normalized (Pearce 1983) multi-element plots (Fig. 5A, B) an increasing enrichment of the high field strength elements is observed relative to MORB from Ti (enrichment factor 1.3–2.0) over Zr (1.6–2.8), Nd (2.1–3.5), Ce (3.2–9.8), La (5.2–8.8) to Nb (5.4–16.2), Ta (9–19) and Th (7–25). Y and the HREEs (Ho-Lu) are close to MORB values. Chondrite normalized REE (Sun 1982) patterns (Fig. 5C) are steep and widely linear between La and Tb but flatten between Tb and Lu. They show no significant Eu anomaly.

Those samples that plot as (non-alkaline) ***tholeiitic basalts and basaltic andesites*** in the Zr/Ti vs. Nb/Y diagram (Fig. 3)

Table 1: Mineralogical composition of selected samples as determined by XRD (numbers in wt.%).

Sample	LAM-1A	LAM-1D	LAM-2N	LAM-3A	LAM-4A	LAM-4G	ERZ-1A	ERZ-2A	ASC-1G	PFE-1A	PFE-1J
Quartz	13	19	11	17	–	14	0.5	1	15	11	13
Plagioclase	–	–	–	0.5*	–	–	61*	46	29	35	15
K-Feldspar	25	–	–	2	23	–	–	–	–	–	–
Clinopyroxene (Augite)	–	–	–	–	–	–	–	14	–	–	–
Ca-Amphibole	–	–	–	–	–	–	–	–	–	–	–
Na-Amphibole	–	–	–	–	16	–	–	–	–	–	–
Epidote, Clinozoisite	–	–	–	–	–	–	–	–	–	–	–
Chlorite	48	18	68	29	17	23	28	26	49	37	32
Biotite	–	–	–	–	–	–	–	–	–	–	0.9
White Mica (Phengite)	10	53	16	46	39	54	–	–	–	–	–
Calcite	–	–	–	–	2	7	8	8	6	14	31
Magnesite	–	6	–	–	–	–	–	–	–	–	–
Magnetite	0.5	–	–	–	–	–	1	1	0.2	–	–
Hematite	0.8	0.5	–	1	–	–	–	–	0.1	–	3
Ilmenite	–	–	0.5	–	–	0.3	–	–	–	–	–
Rutile, Anatase	2	1	2	1	2	1	2	–	2	0.3	–
Titanite	–	–	–	–	–	–	–	4	–	3	0.9
Apatite	–	–	–	1	–	–	–	–	–	0.7	–
Sulfides (Pyrite, Cpy, …)	<0.1	<0.1	0.6	<0.1	0.5	–	<0.1	<0.1	0.1	–	<0.1
Gypsum	0.7	0.8	–	2	–	–	–	–	–	–	4
APS (Crandallite Group)	0.9	0.6	2	–	–	0.3	–	–	–	–	–

* high Ca-content, fitted with andesine; all others fitted with albite

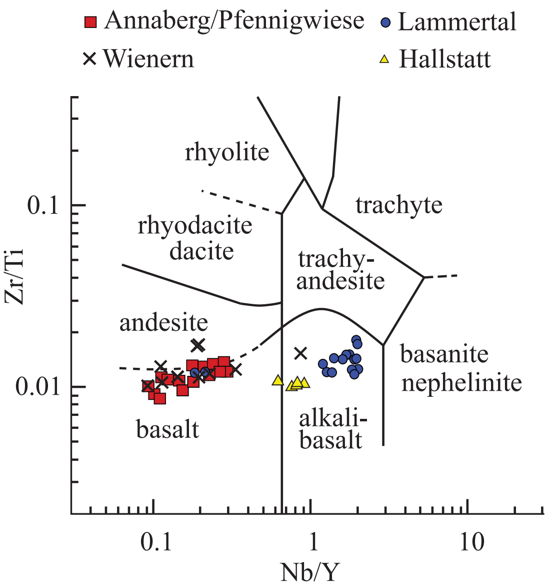

Fig. 3. Nb/Y vs Zr/Ti diagram of Winchester & Floyd (1977) for the discrimination of altered volcanic rocks.

can be divided into two groups based on their MORB-normalized trace element patterns. A first group, mainly represented by the samples from Annaberg and Pfennigwiese, displays flat patterns with MORB normalized values pivoting around 1 (Fig. 5D, E). In the Pearce diagrams of figure 4, these samples plot into the MORB fields. The REE patterns of these samples are also MORB-like (Fig. 5F), although somewhat variable with regard to the LREEs. Sample PFE-1J shows, for example, a slight LREE enrichment, while other samples like PFE-1A yield a slight LREE depletion. The second geochemical group is mainly represented by the samples from the Wienern quarry (Figs. 3, 4, 5G, H, I). At first sight, several analyses from this quarry look MORB-like as well, with MORB-like Nb/Zr, Ti/Zr and Th/Ta ratios. However, in MORB normalized patterns (Fig. 5G, H) almost all samples from Wienern display a characteristic Nb deficiency relative to Ce, which is (with one exception) not observable in the MORB-type samples from Annaberg and Pfennigwiese (group 1). Furthermore, despite of being tholeiitic, many volcanic rocks from Wienern differ from the samples from Annaberg and Pfennigwiese by increased Zr, Ti contents and Zr/Y ratios that fall into the typical range of within-plate basalts (Fig. 4). However, due to low Nb, Ta and Th contents (Fig. 5G, H), the bulk of these samples cannot be addressed as proper within-plate basalt. Only two samples from Wienern (i.e., those that lack the characteristic Ce spike in Fig. 5G) have a reasonable geochemical affinity to within-plate basalt or E-MORB.

The significant enrichment of Ce relative to Nb which is seen in most samples from Wienern, is reminiscent of basalts from subduction settings, but could eventually also result from crustal contamination. Irrespectively of which interpretation is preferred: fact is that the late Permian tholeiitic magmatism in the Wiener quarry is geochemically different from the Permian MORB-like basaltic magmatism of Annaberg and Pfennigwiese. Apart from the significantly different Ce/Nb systematics, it should also be noted that the Wienern quarry exposes a number of remarkably fractionated volcanites with relatively high Zr contents (150–300 ppm), which appear

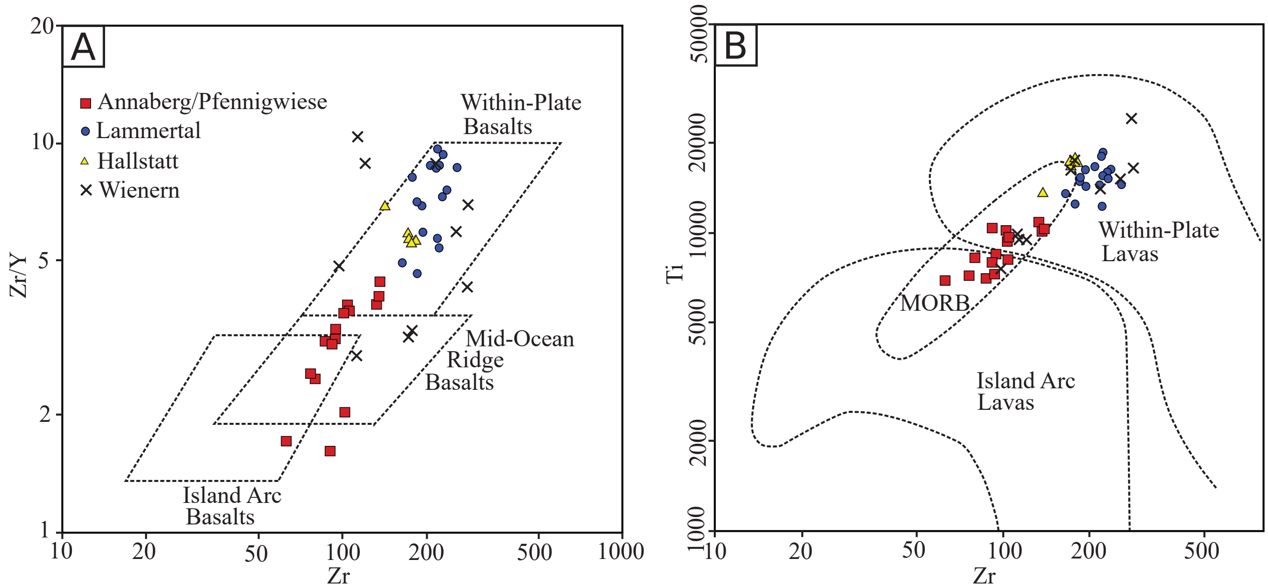

Fig. 4. Trace element plots for the discrimination of basalts according to their tectonic setting. **A** — after Pearce & Norry (1979), **B** — after Pearce (1982).

to be totally missing in the occurrences of Annaberg and Pfennigwiese. Two of these rocks (WIE-31 and WIE-32) plot as andesites in the Zr/Ti vs. Nb/Y diagram of Fig. 3, although their SiO_2 (45–48 wt.%) is in a basaltic rather than andesitic range.

Discussion

Arguments for synsedimentary volcanism in the Haselgebirge formation

As mentioned earlier, the samples to this study were mostly dm-sized isolated rock pieces collected inside mapped Haselgebirge units. However, direct contacts between these volcanites and Haselgebirge sediments are rarely exposed. Thus, a synsedimentary origin of the volcanic rocks could theoretically be challenged and we cannot fully rule out, indeed, that single samples could be derived from tectonic inlayers within the Haselgebirge. This possibility exists particularly for the Pfennigwiese locality, which is part of the Geyerstein mélange, a tectonic shear zone, which includes single (Triassic?) serpentinite bodies (Strauss et al. 2023).

However, overall, we favour a model of synsedimentary volcanism based on the following reasons:

- Synsedimentary contacts between lava flows and evaporates undoubtedly exist and are well exposed in the salt mine Hallstatt (Leitner et al. 2017).
- Volcanic rocks from the Moosegg location were dated at a late Permian formation age (Schorn et al. 2013) .
- Tectonic xenoliths sheared into the evaporite body are infrequent and the few proven examples are several meters large and easily recognized.
- Triassic limestone, the typical country rock, is hardly found as tectonic inlayer, which implies that tectonic admixtures play little role in the Haselgebirge unit.
- The strong alteration of the volcanic samples, partly with uptake of sulfur, can most easily be understood in a warm synsedimentary contact situation of lavas (perhaps also tuffs) and evaporitic sediments.

Message of the geochemical data

Two results of this study came particularly unexpected and deserve a more in-depth discussion: The first is that the Permian volcanism in the Haselgebirge Formation has turned out to be almost exclusively basaltic. Intermediate and felsic volcanites (andesites, dacites, rhyolites) apparently play no appreciable role in this formation. This is, at least at first sight, surprising, considering the fact that granitic to rhyolitic magmatism of Permian age is widely reported from all over the Alps and Carpathians (Ivan et al. 2002; Finger et al. 2003; Schuster & Stüwe 2008; Radvanec et al. 2009; Petri et al. 2017; Plašienka 2018; Villaseñor et al. 2021; Neubauer et al. 2022). However, after screening the published geochronological dates, leaving imprecise and ambiguous ones aside, we can specify that felsic, Permian magmatism in the Austroalpine Unit had its climax in the middle Permian and obviously decreased in intensity towards the late Permian (see data compilation in Neubauer et al. 2022; Knoll et al. 2023). The entirely basic volcanism in the Haselgebirge shows that, towards the end of the Permian, crustal melting has lost importance as a magma forming process relative to mantle magmatism.

This changing character of magmatism is likely a reflection of ongoing crustal thinning. While during the mid Permian,

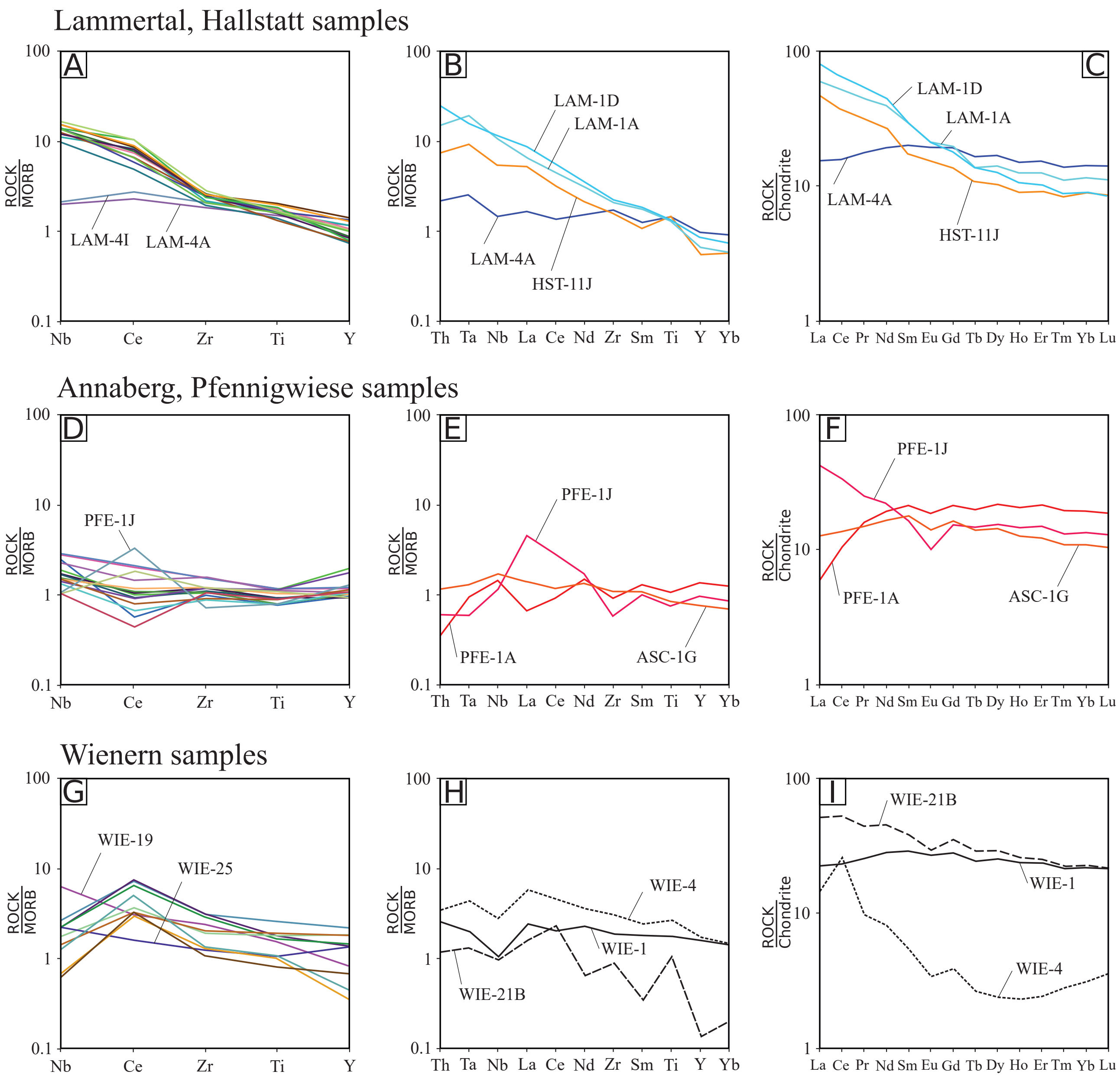

Fig. 5. MORB-normalized multi-element plots (Pearce 1983) and CHONDRITE normalized REE patterns (Sun 1982). Diagrams A, D, G are based on the XRF data from Tables 2–4; diagrams B, C, E, F, H, I are based on ICP-MS data from Table 5.

extension was probably diffusely distributed over the continental lithosphere, it seems to have focused in the late Permian into a narrow rift area with strongly attenuated crust in which only basaltic magmatism occurred. Deep normal faulting may have led to a passive mantle upwelling underneath this pre-Meliata rift (Schorn et al. 2013; Huang et al. 2022). However, also elsewhere in the Austroalpine, the production of felsic crustal melts may have decreased in the late Permian, because the magmatically fertile parts of the crust were largely transferred into infertile granulite during the voluminous middle Permian granite forming event.

Compared to the probably relatively localized late Permian pre-Meliata rift, the middle Permian thermal event likely had a much larger regional extent. Indeed, granitic intrusions of middle Permian age are not only observed in many parts of the Austroalpine realm (Neubauer et al. 2022), but also in the northwards adjacent sub-Penninic basement (e.g., von Quadt et al. 1999; Eichhorn et al. 2000). Thus, we hypothesize that the lithospheric mantle layer underneath the Austroalpine Pangea segment (and neighboring Pangea areas?) was already strongly thinned out at that time by thermal erosion. This middle Permian cannibalism of the mantle lithosphere did,

Table 2: XRF analyses of volcanic samples from the Annaberg/Pfennigwiese.

Sample	ASC-1D	ERZ-2A	PFE-1B	PFE-1A	ASC-1G	ASC-1B	PFE-2A	PFE-1J	ERZ-2D	ERZ-1B	ERZ-2B	ERZ-3A	ERZ-1A	LAS-1B	LAS-1A
Major Elements (wt.%, normalized to 100)															
SiO_2	48.17	48.82	48.20	50.62	53.32	54.78	49.39	44.97	49.31	44.51	48.26	48.63	44.01	48.15	49.16
Al_2O_3	16.24	16.32	15.44	15.49	15.82	15.45	16.89	14.40	17.92	18.19	17.04	18.16	18.09	19.62	18.94
MnO	0.19	0.24	0.27	0.25	0.17	0.15	0.26	0.29	0.23	0.61	0.26	0.21	0.55	0.20	0.25
MgO	9.92	9.28	8.44	7.83	9.74	9.07	8.57	8.46	8.13	10.38	10.24	10.86	11.71	9.68	9.77
CaO	5.76	6.55	11.14	9.54	3.76	3.62	8.79	13.76	7.26	9.50	5.85	6.11	9.00	5.31	4.12
Na_2O	3.02	4.65	3.59	3.96	3.17	3.46	3.95	3.27	4.88	3.04	4.14	3.29	2.76	3.82	4.99
K_2O	<0.1	0.23	0.29	0.35	<0.1	<0.1	1.17	1.15	0.13	0.26	0.38	0.39	0.22	0.38	0.39
TiO_2	1.28	1.74	1.66	1.61	1.30	1.35	1.32	1.11	1.63	1.54	1.61	1.15	1.51	1.12	1.15
P_2O_5	0.10	0.19	0.11	0.12	0.13	0.12	0.11	<0.1	0.21	0.10	0.21	<0.1	0.10	0.10	<0.1
Fe_2O_3	14.90	11.49	10.47	9.86	12.12	11.54	9.20	11.82	9.89	11.38	11.47	10.73	11.52	11.17	10.82
SO_3	<0.1	0.16	<0.1	<0.1	<0.1	<0.1	<0.1	0.41	<0.1	0.14	0.19	<0.1	0.16	<0.1	<0.1
F	0.23	0.17	0.18	0.19	0.19	0.19	0.19	0.18	0.18	0.21	0.19	0.19	0.21	0.16	0.15
Trace Elements (ppm)															
Ba	34	55	22	43	106	146	45	37	39	51	91	157	55	124	89
Ce	14	30	20	19	20	19	18	42	29	28	24	17	21	16	21
Cl	206	140	216	234	373	247	148	84	161	68	196	100	52	148	137
Co	31	40	33	17	37	30	13	10	41	55	40	46	50	44	44
Cr	338	237	290	279	501	449	435	265	256	370	261	279	395	240	246
Ga	15	16	18	17	13	13	14	17	16	18	17	17	20	18	16
Nb	3	9	6	5	6	6	5	4	10	4	8	4	5	8	5
Ni	113	82	96	79	94	90	130	126	77	194	80	122	186	133	133
Rb	3	4	6	6	3	3	15	25	3	5	7	15	5	9	12
Sc	40	34	50	52	42	49	27	39	36	44	34	42	42	35	39
Sr	103	265	124	108	192	225	98	53	511	156	316	152	152	1147	320
V	290	285	445	423	242	224	252	422	260	237	271	183	246	188	185
Y	30	35	57	50	27	29	32	37	34	28	31	30	28	28	29
Zn	148	83	67	65	135	138	65	42	77	136	72	64	143	95	79
Zr	91	133	91	102	104	95	80	63	135	104	135	77	103	87	93

Table 3: XRF analyses of volcanic samples from Lammertal.

Sample	MOO-3	LAM-4I	LAM-4G	LAM-4D	LAM-4A	LAM-3G	LAM-3F	LAM-3B	LAM-3D	LAM-2E	LAM-2F	LAM-2N	LAM-1A	LAM-1D	LAM-1F	LAM-1G
Major Elements (wt.%, normalized to 100)																
SiO_2	49.33	50.80	53.72	48.23	47.86	50.79	47.43	47.75	47.03	42.76	45.74	41.85	46.66	53.28	44.53	43.51
Al_2O_3	16.98	17.46	19.35	19.07	15.82	19.72	18.63	17.58	19.16	21.03	20.25	20.66	17.60	19.70	21.42	21.84
MnO	0.15	<0.1	0.10	<0.1	<0.1	<0.1	0.10	<0.1	<0.1	<0.1	<0.1	<0.1	<0.1	<0.1	<0.1	<0.1
MgO	9.77	9.31	11.41	14.18	9.46	14.15	10.67	10.25	10.63	19.16	16.58	22.61	19.26	12.07	16.55	21.04
CaO	5.83	1.80	0.23	0.32	0.91	<0.1	2.86	9.45	2.66	<0.1	0.14	<0.1	0.91	0.11	<0.1	<0.1
Na_2O	2.45	0.12	<0.1	<0.1	0.88	<0.1	0.80	<0.1	0.74	<0.1	<0.1	<0.1	<0.1	<0.1	<0.1	<0.1
K_2O	4.41	9.58	5.09	3.40	7.04	4.02	6.46	4.08	6.50	2.90	3.36	1.90	1.89	4.69	3.31	3.56
TiO_2	2.39	2.45	2.42	2.67	2.17	2.36	2.92	2.49	2.98	2.57	2.31	2.61	2.00	1.96	2.31	2.62
P_2O_5	0.59	0.28	0.16	0.12	0.22	<0.1	0.62	0.18	0.62	<0.1	0.18	0.14	0.11	0.14	0.13	<0.1
Fe_2O_3	7.79	7.47	6.60	9.95	11.37	7.55	8.92	7.62	9.04	10.77	10.77	9.03	9.54	7.19	11.13	6.77
SO_3	<0.1	0.35	0.51	1.51	3.87	0.82	0.20	0.12	0.15	0.22	0.19	0.46	1.51	0.34	<0.1	<0.1
F	<0.1	0.15	0.18	0.24	0.18	0.18	0.23	0.20	0.22	0.24	0.20	0.35	0.19	0.22	0.25	0.31
Trace Elements (ppm)																
Ba	389	29	218	63	63	314	255	64	231	30	55	57	498	49	52	62
Ce	75	37	88	113	32	108	98	69	93	87	85	123	59	75	92	83
Cl	556	235	157	192	167	101	158	90	147	210	160	192	503	319	185	128
Co	36	35	25	10	21	16	21	7	22	21	31	19	15	8	9	4
Cr	324	225	200	359	213	176	132	361	148	109	502	208	458	95	545	470
Ga	21	18	22	20	19	21	23	20	22	24	22	23	18	19	20	25
Nb	47	7	54	47	7	57	52	49	53	46	41	52	34	43	38	42
Ni	140	81	80	136	93	64	72	103	73	75	161	96	146	53	200	111
Rb	74	39	140	148	66	127	100	192	104	68	105	41	53	147	106	89
Sc	32	36	22	32	36	23	23	25	31	21	34	21	26	16	28	35
Sr	138	26	113	290	20	507	56	147	51	465	185	1604	122	957	36	51
V	313	297	279	303	304	261	280	285	284	209	284	173	236	181	278	313
Y	26	40	31	24	33	29	38	25	41	25	25	28	22	23	33	31
Zn	129	39	141	16	71	33	82	82	78	37	69	23	37	9	19	32
Zr	185	184	227	206	164	255	217	220	222	229	215	193	178	218	194	235

Table 4: XRF analyses of volcanic samples from Wienern.

Sample	WIE-4	WIE-2	WIE-1	WIE-19	WIE-21A	WIE-21B	WIE-25	WIE-30	WIE-31	WIE-32	WIE-3
Major Elements (wt.%, normalized to 100)											
SiO_2	49.82	49.01	48.75	49.32	46.16	49.61	40.91	48.92	47.88	45.32	47.97
Al_2O_3	14.27	14.10	13.08	17.96	21.99	22.37	17.30	17.70	17.85	16.93	3.00
MnO	<0.1	0.15	0.15	<0.1	0.13	<0.1	0.27	0.10	<0.1	<0.1	0.14
MgO	8.41	8.71	8.07	6.97	6.01	4.93	17.06	14.63	8.45	8.61	40.01
CaO	1.66	4.69	5.00	5.35	5.53	2.50	4.17	0.33	2.48	3.50	0.16
Na_2O	0.64	1.67	2.80	1.08	0.44	1.08	1.72	<0.1	1.39	1.33	<0.1
K_2O	7.07	5.27	4.43	8.70	9.46	9.52	0.57	10.85	7.93	7.53	<0.1
TiO_2	3.90	2.78	2.59	2.25	1.53	1.52	1.58	1.21	2.42	2.64	0.10
P_2O_5	0.59	0.25	0.23	0.37	<0.1	0.11	0.17	<0.1	0.32	0.42	<0.1
Fe_2O_3	12.11	12.54	13.92	6.96	5.81	7.00	15.71	5.24	7.55	8.19	7.74
SO_3	1.11	0.52	0.67	0.59	2.41	0.78	0.14	0.57	3.30	5.10	0.27
F	0.18	0.14	0.14	0.26	0.21	0.28	0.18	0.13	0.21	0.21	<0.1
Trace Elements (ppm)											
Ba	25	54	23	67	518	568	27	48	73	56	12
Ce	81	42	46	40	60	40	26	42	74	84	24
Cl	153	351	231	176	366	206	128	588	107	106	155
Co	20	33	40	20	7	9	31	11	21	21	127
Cr	221	66	89	226	627	628	644	517	256	252	3597
Ga	22	22	22	18	19	20	20	18	23	23	8
Nb	9	5	6	21	4	2	8	2	8	8	1
Ni	43	41	44	87	162	105	236	241	127	129	2820
Rb	104	37	37	238	109	104	12	50	68	77	3
Sc	57	46	48	23	39	32	43	23	32	31	16
Sr	63	86	109	76	113	87	245	67	41	52	17
V	449	468	442	223	310	354	288	170	275	295	82
Y	65	53	54	24	13	11	39	20	43	40	2
Zn	61	123	139	53	47	50	418	491	130	140	955
Zr	278	177	171	215	120	113	112	97	253	281	21

however, not result in an immediate rifting of the overlying crust, but it has prepared the stage for the subsequent Meliata rift formation and presumably also for the later opening of the Penninic ocean.

Notably, neither the middle Permian granite forming event nor the late Permian mafic magmatism in the Austroalpine have analogues in the Variscides north of the Alpine front. Therefore, these magmatic events cannot be explained merely in terms of a general thinning of the central European Pangea crust. Apparently, there must have been a tectonic cause of regional nature – related to Paleotethys subduction (Stampfli et al. 2013) or the opening of the Neotethys (van Hinsbergen et al 2020).

Apart from the important notation that the Haselgebirge volcanism is overall basaltic and more or less devoid of intermediate and felsic members, this study highlights for the first time regional geochemical variations of this basaltic volcanism as a second major result.

(i) Volcanic rocks exposed in the eastern locations of the Haselgebirge Formation (Annaberg and Pfennigwiese) have overwhelmingly MORB-like geochemistry.

(ii) The sampling area Lammertal in the west is characterized by alkali-basaltic volcanism and

(iii) the sampling site Wienern yielded mainly distinct low-Nb basalts.

Obviously, different volcanic eruption centers existed in the Haselgebirge realm that were fed from different magma sources. Given the severe alteration-related geochemical changes in the available samples, a detailed modeling of magma evolutions is not attempted here. Nevertheless, some more general petrogenetic conclusions can be tentatively drawn. A first concerns the MORB-like volcanism in the east (Annaberg and Pfennigwiese), which can reasonably be explained in terms of a depleted asthenospheric peridotite source that melted upon decompression. It is possible that the Haselgebirge MORBs are the extrusive products of the gabbroic-basaltic magmatic complex in the Austroalpine Koralpe region, which according to Chang et al. (2023), remained active until the latest Permian/early Triassic (cf. model in Fig. 6).

A puzzling question is why the volcanism in the western Haselgebirge Formation does not show the same MORB-like characteristics as in Annaberg and Pfennigwiese, and why there is a clear dominance of alkali-basaltic volcanic rocks in that area. The petrogenesis and tectonic meaning of alkali-basalts is controversial (see e.g., Pilet et al. 2011; Xia & Li 2019; Mesa & Lange 2021). However, it is a matter of fact that, apart from ocean islands, alkali-basaltic rocks are particularly often reported from continental rift settings (Harangi 1994; Xu et al. 2020). According to Pilet et al. (2011),

Table 5: LA-ICP-MS analyses for selected samples.

Sample	HST-11J	LAM-1A	LAM-1D	LAM-4A	WIE-1	WIE-4	WIE-21B	PFE-1A	PFE-1J	ASC-1G
Parts per million										
Li	208.8	139.9	84.2	74.5	89.0	76.7	159.8	65.4	63.0	76.7
Be	1.5	1.2	2.4	1.6	0.9	2.7	2.4	0.3	0.4	0.5
Be	60.8	14.1	36.4	16.9	38.4	48.8	235.5	10.8	11.9	4.5
Al	71909.9	83194.5	110845.7	80543.3	70293.5	65293.8	72636.2	72125.3	71320.8	85102.2
Ca	40039.3	3452.4	920.1	3723.9	20007.8	6751.3	6312.1	32111.8	38434.2	14287.0
Sc	22.0	23.5	19.5	32.3	41.8	39.4	18.5	40.2	33.4	38.0
Ti	13066.4	12462.1	11331.3	12109.0	15571.6	24109.2	8675.7	8940.4	6482.2	7983.1
V	232.6	214.6	169.1	268.0	441.4	455.7	300.2	364.0	378.7	201.4
Cr	20.4	360.9	85.9	168.7	57.9	158.0	521.3	207.1	203.3	295.7
Mn	275.6	267.5	203.8	578.6	1187.3	552.6	390.6	1820.1	1765.3	1132.0
Fe	48380.1	69842.4	52922.6	77375.8	92939.3	77250.8	42968.6	61584.6	82749.3	75173.2
Co	5.8	19.1	10.2	24.3	41.4	21.6	5.4	17.7	8.2	29.2
Ni	17.5	130.0	44.5	79.6	36.3	34.2	88.0	65.0	107.5	69.8
Cu	15.4	5.2	1.7	1.2	12.7	3.1	0.2	30.6	1.4	282.4
Zn	31.7	26.9	24.9	53.7	117.7	49.6	42.6	44.0	34.1	109.2
Ga	15.4	18.9	23.0	18.4	21.0	22.1	19.2	15.0	16.9	11.7
Ge	0.1	0.2	0.3	0.2	0.2	0.2	0.1	0.1	0.1	0.1
As	17.1	8.8	11.6	8.8	6.8	11.5	2.7	14.1	5.7	11.6
Rb	30.3	51.0	141.7	62.9	34.0	60.4	48.4	3.5	21.6	1.5
Sr	116.3	126.3	1033.5	15.7	107.1	57.4	46.2	107.4	39.0	203.8
Y	16.7	20.2	25.6	28.9	46.3	50.6	3.8	41.1	28.8	23.3
Zr	143.9	186.8	201.8	153.6	167.1	272.0	76.7	83.0	51.6	97.2
Nb	18.8	36.9	39.5	5.0	3.6	9.5	3.3	1.0	0.7	2.8
Mo	1.5	2.6	0.7	0.6	0.6	1.8	0.2	0.1	0.2	0.1
Ag	0.1	0.1	0.2	0.1	0.1	0.2	0.1	0.1	0.0	0.1
Cd	b.d.l.	b.d.l.	b.d.l.	0.8	b.d.l.	b.d.l.	b.d.l.	b.d.l.	b.d.l.	b.d.l.
Sn	1.5	1.7	2.2	1.6	1.7	2.6	1.1	1.0	0.5	1.2
Sb	1.2	2.4	3.3	1.2	0.6	4.1	1.0	0.2	0.3	0.2
Cs	5.6	0.9	2.7	4.0	3.6	3.9	5.1	0.2	0.7	0.3
Ba	26.6	569.3	44.7	67.6	39.6	44.9	339.3	34.2	41.7	103.2
La	15.5	19.6	26.2	5.0	7.2	16.9	4.7	2.0	13.8	4.2
Ce	32.0	45.0	56.0	13.6	20.1	44.6	22.4	9.1	28.7	11.8
Pr	4.1	5.7	7.0	2.3	3.3	5.8	1.3	2.1	3.2	1.9
Nd	17.0	24.8	28.3	12.2	17.8	28.2	5.1	12.1	13.7	10.4
Sm	3.5	5.9	6.1	4.1	5.8	7.8	1.1	4.3	3.4	3.6
Eu	1.2	1.6	1.6	1.5	2.1	2.3	0.3	1.4	0.8	1.1
Gd	3.8	4.9	5.4	5.3	7.7	9.6	1.1	5.9	4.2	4.5
Tb	0.5	0.7	0.7	0.8	1.2	1.4	0.1	1.0	0.7	0.7
Dy	3.5	4.3	4.8	5.8	8.7	9.9	0.8	7.5	5.2	4.9
Ho	0.7	0.8	1.0	1.2	1.8	2.0	0.2	1.6	1.1	1.0
Er	2.1	2.3	2.8	3.4	5.3	5.6	0.5	4.8	3.4	2.8
Tm	0.3	0.3	0.4	0.5	0.8	0.8	0.1	0.7	0.5	0.4
Yb	1.9	2.0	2.5	3.1	4.8	4.9	0.7	4.3	2.9	2.4
Lu	0.3	0.3	0.4	0.5	0.7	0.7	0.1	0.6	0.4	0.4
Hf	3.3	4.2	4.8	3.8	4.4	6.4	2.1	2.4	1.7	2.5
Ta	1.7	3.4	2.9	0.5	0.4	0.8	0.2	0.2	0.1	0.2
W	1.0	1.9	1.6	0.4	0.1	0.6	2.2	0.6	1.8	0.8
Tl	0.1	0.1	0.1	0.3	0.3	0.3	0.7	b.d.l.	0.1	b.d.l.
Pb (206)	1.8	1.2	2.7	5.0	2.4	5.8	0.7	0.7	0.7	0.7
Pb (208)	1.6	1.1	2.5	4.9	2.4	5.6	0.6	0.7	0.6	0.7
Bi	b.d.l.	b.d.l.	0.1	0.1	b.d.l.	b.d.l.	b.d.l.	b.d.l.	b.d.l.	b.d.l.
Th	1.5	3.0	5.0	0.4	0.5	0.7	0.2	0.1	0.1	0.2
U	1.2	1.7	3.5	0.2	0.2	1.7	0.5	0.2	1.1	0.1

alkali-basaltic magmas can form in such settings through remelting of distinct hornblende-bearing domains within the lithospheric mantle, which were metasomatically created adjacent to magmatically active asthenosphere. This model seems quite attractive for the Haselgebirge volcanism: Based on the partly MORB-like magmatism we envisage that asthenospheric mantle updoming and thermal erosion of preexisting Pangea lithosphere had occurred (Fig. 6). The sub-Pangea

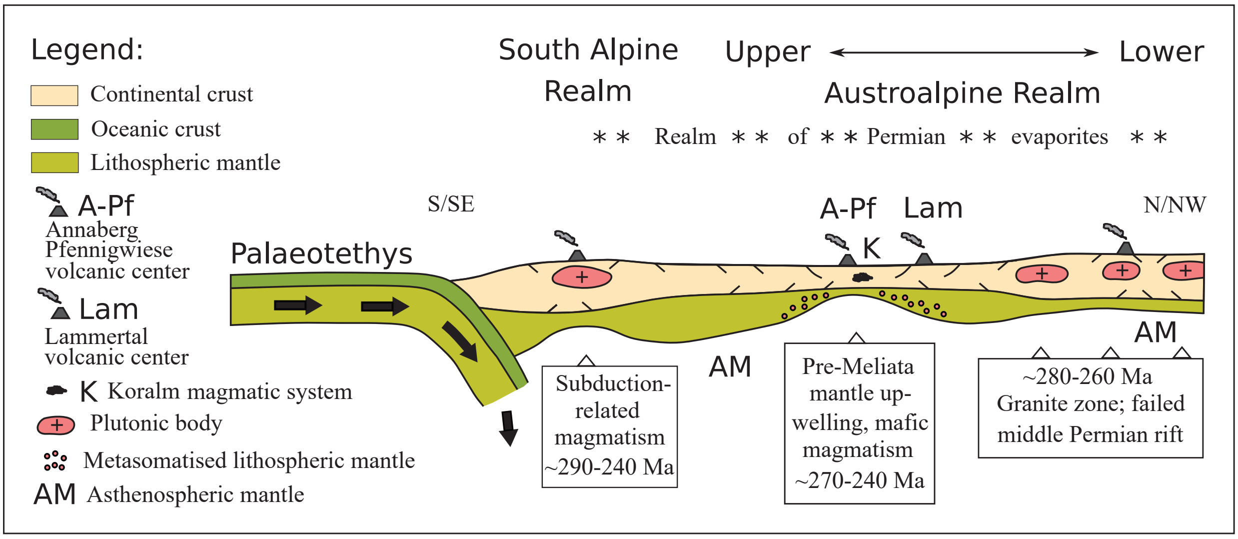

Fig. 6. Sketch showing the possible geodynamic situation at ca. 250 Ma during the deposition of the Haselgebirge Formation (partly based on a model of Huang et al. 2022, which involves the subduction of the Paleotethys in the sense of Stampfli 1996, and Stampfli & Mosar 1999). For further explanations, see Discussion.

lithospheric mantle that adjoined to magmatically active asthenosphere may have been metasomatized (hornblendized). Further heat input from the upwelling mantle may have subsequently caused melting of this metasomatized zone with the formation of alkali-basaltic magmas. The observed geochemical variation of the volcanic rocks in the Haselgebirge Formation could thus be very conveniently interpreted in terms of a hot, late Permian, passive mantle upwelling in the east, which bordered and interacted with lithospheric sub-Pangea mantle towards west. In that sense, the striking east-west asymmetry of Permian volcanism in the Haselgebirge (MORB vs. alkali-basaltic) prescribes, in a way, the later geometry of the Meliata ocean: notably, there are clearly more traces of this ocean found in the western Carpathians than in the Alps, suggesting its continuous narrowing towards west (Ivan 2002; Putiš et al. 2019).

More difficult to interpret in terms of their petrogenesis are the low-Nb basalts from the quarry Wienern. Nb deficiencies in basalts (relative to similarly incompatible trace elements like La or Th) do quite often result from assimilation of crustal material (e.g., Yu et al. 2022) and this may be one possible explanation also for the volcanic rocks of Wienern. On the other hand, it can be seen in the data set from Wienern that the negative Nb anomalies are equally great in samples that represent a primitive low-Zr magma and in samples that represent fractionated high-Zr basaltic magma (Fig. 5G). This would imply that a Nb deficiency had already existed in the primary mantle magmas (e.g., Lustrino et al. 2019; Casetta et al. 2021). Thus, a relict subduction modified mantle domain perhaps may have played a role in the petrogenesis of the Wienern volcanic samples. Latest research shows that a possible inherited subduction signature occurs also in (Triassic?) serpentinite rocks next to the location Pfennigwiese (Strauss et al. 2023).

Conclusions

The break-up of the Pangea continent in the Permian led to a distinct succession of magmatic events in the Austrian Alps (Austroalpine Unit). In the early to mid Permian period granitic/rhyolitic magmatism, attributed to lower crustal melting, was widespread. During the late Permian, basaltic magmatism gained importance. Its partly MORB-like characteristics is indicative of a (passive?) mantle upwelling. This late Permian, probably still sub-continental mantle upwelling preluded the early Triassic opening of the Meliata ocean. Late Permian alkali-basaltic magmatism in the western part of the Upper Austroalpine Haselgebirge Formation is interpreted as being derived from metasomatized (hornblendized) lithospheric mantle, that had formed around magmatically active asthenospheric mantle domains, in the sense of the model of Pilet et al. (2011). The observed source variations within the Haselgebirge basaltic volcanism may point to a comparably greater degree of lithosphere thinning in the east. A subduction modified mantle source may have been locally involved in the Permotriassic magmatism in the Alps (locality Höflein, Strauss et al. 2023; locality Wienern, this study). Whether this is an inherited feature from a remnant Variscan mantle or indicative for coeval subduction of the Paleotethys in the sense of Stampfli et al. (2013) remains an open question at the present state of investigation.

Acknowledgements: This research did not receive any specific grant from funding agencies in the public, commercial, or not-for-profit sectors. We thank reviewers Ulrich Glasmacher and Ralf Schuster for constructive comments and the chief editor of Geologica Carpathica Igor Broska for the editorial handling of this paper.

References

Bergmann J., Friedel P. & Kleeberg R. 1998: BGMN – a new fundamental parameters based Rietveld program for laboratory X-ray sources, its use in quantitative analysis and structure investigations. *CPD Newsletter* 20, 5–8.

Berra F. & Felletti F. 2011: Syndepositional tectonics recorded by soft-sediment deformation and liquefaction structures (continental Lower Permian sediments, southern Alps, northern Italy): Stratigraphic significance. *Sedimentary Geology* 235, 249–263. https://doi.org/10.1016/j.sedgeo.2010.08.006

Binder T., Marks M.A.W., Walter B.F., Wenzel T. & Markl G. 2024: Two Distinct Metasomatized Mantle Sources Produced Two Groups of Alkaline SiO_2-Undersaturated Rocks in the Southern Central European Volcanic Province. *Journal of Petrology* 65, egae070. https://doi.org/10.1093/petrology/egae070

Casetta F., Ickert R.B., Mark D.F., Giacomoni P.P., Bonadiman C., Ntaflos T., Zanetti A. & Coltorti M. 2021: The Variscan subduction inheritance in the Southern Alps Sub-Continental Lithospheric Mantle: Clues from the Middle Triassic shoshonitic magmatism of the Dolomites (NE Italy). *Lithos* 380–381, 105856. https://doi.org/10.1016/j.lithos.2020.105856

Chang R., Neubauer F., Liu Y., Genser J., Jin W., Yuan S., Guan Q., Huang Q. & Li W. 2020: Subduction of a rifted passive continental margin: the Pohorje case of Eastern Alps–constraints from geochronology and geochemistry. *Swiss Journal of Geosciences* 113, 14. https://doi.org/10.1186/s00015-020-00369-z

Chang R., Neubauer F., Liu Y., Genser J., Guan Q., Huang Q. & Yuan S. 2023: Permian to Triassic protolith ages of type locality eclogites in the Eastern Alps: Implications for the opening of the Meliata back-arc basin. *Geology* 51, 537–542. https://doi.org/10.1130/G50903.1

Döbelin N. & Kleeberg R. 2015: Profex: a graphical user interface for the Rietveld refinement program BGMN. *Journal of Applied Crystallography* 48, 1573–1580.

Eichhorn R., Loth G., Höll R., Finger F., Schermaier A. & Kennedy A. 2000: Multistage Variscan magmatism in the central Tauern Window (Austria) unveiled by U/Pb SHRIMP zircon data. *Contributions to Mineralogy and Petrology* 139, 418–435.

Faupl P. 1970: Zur Geologie des NW-Abschnitts des Wechselgebietes zwischen Trattenbach (NÖ) und Fröschnitz (Stmk.) – Österreich. *Mitteilungen der Gesellschaft der Geologie und Bergbaustudenten Wien* 19, 27–70.

Fernandez O.,·Ortner H.,·Sanders D.,·Grasemann B. &·Leitner T. 2024: Salt-rich versus salt-poor structural scenarios in the central Northern Calcareous Alps: implications for the Hallstatt facies and early Alpine tectonic evolution (Eastern Alps, Austria). *International Journal of Earth Sciences* 113, 245–283. https://doi.org/10.1007/s00531-023-02377-4

Finger F., Broska I., Haunschmid B., Hraško Ľ., Kohút M., Krenn E., Petrík I., Riegler G. & Uher P. 2003: Electron-microprobe dating of monazites from western Carpathian basement granitoids: Plutonic evidence for an important Permian rifting event subsequent to Variscan crustal anatexis. *International Journal of Earth Sciences* 92, 86–98. https://doi.org/10.1007/s00531-002-0300-0

Gawlick H.J. & Missoni S. 2015: Middle Triassic radiolarite pebbles in the Middle Jurassic Hallstatt Melange of the Eastern Alps: implications for Triassic-Jurassic geodynamic and paleogeographic reconstructions of the western Tethyan realm. *Facies* 61, 13. https://doi.org/10.1007/s10347-015-0439-3

Granado P., Roca E., Strauss P., Pelz K. & Muñoz J.A. 2019: Structural styles in fold-and-thrust belts involving early salt structures: the Northern Calcareous Alps (Austria). *Geology* 47, 51–54. https://doi.org/10.1130/G45281.1

Gruber P., Faupl P. & Koller F. 1992: Zur Kenntnis basischer Vulkanitgerölle aus Gosaukonglomeraten der östlichen Kalkalpen – ein Vergleich mit Vulkaniten aus dem Haselgebirge. *Mitteilungen der Österreichischen Geologischen Gesellschaft* 84, 77–100.

Haas J., Kovács S., Krystyn L. & Lein R. 1995: Significance of Late Permian–Triassic facies zones in terrane reconstruction in the Alpine–North Pannonian domain. *Tectonophysics* 242, 19–40. https://doi:10.1016/0040-1951(94)00157-5

Habler G., Thöni M. & Miller C. 2007: Major and trace element chemistry and Sm–Nd age correlation of magmatic pegmatite garnet overprinted by eclogite-facies metamorphism. *Chemical Geology* 241, 4–22.

Harangi S. 1994: Geochemistry and petrogenesis of the Early Cretaceous continental rift-type volcanic rocks of the Mecsek Mountains, South Hungary. *Lithos* 33, 303–321.

Horváth P. 2000: Metamorphic evolution of gabbroic rocks of the Bódva valley ophiolite complex, NE Hungary. *Geologica Carpahica* 51, 121–129.

Huang Q., Neubauer F., Liu Y., Genser J., Guan. Q., Chang R., Yuan S. & Yu S. 2022: Permian-Triassic granites of the Schladming complex (Austroalpine basement): Implications for subduction of the Paleo-Tethys Ocean in the Eastern Alps. *Gondwana Research* 109, 205–224. https://doi.org/10.1016/j.gr.2022.05.006

Hubmann B., Ebner F., Ferretti A., Kido E., Krainer K., Neubauer F., Schönlaub H.P. & Suttner T.J. 2014: The Paleozoic Era(them). *Abhandlungen der Geologischen Bundesanstalt* 66, 1–135.

Ivan P. 2002: Relics of the Meliata Ocean crust: Geodynamic implications of mineralogical, petrological and geochemical proxies. *Geologica Carpathica* 53, 245–256.

Ivan P., Demko R., Rojkovič I. & Vozár J. 2002: Geochemistry and geodynamic setting of the Permian volcanism in the Western Carpathians: a review. Geologica Carpathica 53, special issue: Proceedings of XVII. Congress of Carpathian-Balkan Geological Association, Bratislava, September 1–4, 2002.

Knoll T., Huet B., Schuster R., Mali H., Ntaflos T. & Hauzenberger C. 2023: Lithium pegmatite of anatectic origin-A case study from the Austroalpine Unit Pegmatite Province (eastern European Alps): geological data and geochemical model. *Ore Geology Reviews* 154, 105298. https://doi.org/10.1016/j.oregeorev.2023.105298

Kozur H. 1991: The evolution of the Meliata-Hallstatt ocean and its significance for the early evolution of the eastern Alps and Western Carpathians. *Palaeogeography, Palaeoclimatology, Palaeoecology* 87, 109–135. https://doi.org/10.1016/0031-0182(91)90132-B

Krainer K. 1993: Late- and post-Variscan sediments of the Eastern and Southern Alps. In: Raumer J.v., Neubauer F. (Eds.): Pre-Mesozoic Geology in the Alps. *Springer*, Berlin, 537–564.

Kralik M., Koller F. & Pober E. 1984: Geochemie und K–Ar – Alter der Diabasvorkommen von Annaberg (Nördliche Kalkalpen, Niederösterreich). *Mitteilungen der Österreichischen Mineralogischen Gesellschaft* 77, 37–55.

Kirchner E.C. 1979: Pumpellyitführende Kissenlavabreccien in der Gips-Anhydrit-Lagerstätte von Wienern am Grundlsee, Steiermark. *Tschermaks Mineralogische und Petrographische Mitteilungen* 26, 149–162.

Kirchner E.C. 1980: Vulkanite aus dem Permoskyth der Nördlichen Kalkalpen und ihre Metamorphose. *Mitteilungen der Österreichen Geologischen Gesellschaft* 71/72, 385–396.

Leitner C. & Spötl C. 2017: The Eastern Alps: Multistage Development of Extremely Deformed Evaporites. In: Soto J.I., Flinch J.F., Tari G. (Eds.): Permo-Triassic Salt Provinces of Europe, North Africa and the Atlantic Margins. *Elsevier*, Amsterdam, 467–482.

Leitner C., Wiesmaier S., Köster M.H., Gilg H.A., Neubauer F. & Finger F. 2017: Alpine halite-mudstone-polyhalite tectonite: Sedimentology and early diagenesis of evaporites in an ancient rift setting (Haselgebirge Formation, eastern Alps). *GSA Bulletin* 129, 1537–1553. https://doi.org/10.1130/B31747.1

Lustrino M., Abbas H., Agostini S., Caggiati M., Carminati E. & Gianolla P. 2019: Origin of Triassic magmatism of the Southern Alps (Italy): constraints from geochemistry and Sr–Nd–Pb isotopic ratios. *Gondwana Research* 75, 218–238. https://doi.org/10.1016/j.gr.2019.04.011

Mandl G.W. & Ondrejičková A. 1991: Über eine triadische Tiefwasserfazies (Radiolarite, Tonschiefer) in den Nördlichen Kalkalpen – Ein Vorbericht: *Jahrbuch der Geologischen Bundesanstalt* 134, 309–318.

McCann T., Pascal C., Timmerman M.J., Krzywiec P., López-Gómez J., Wetzel L., Krawczyk C.M., Rieke H. & Lamarch J. 2006: Post-Variscan (end Carboniferous-Early Permian) basin evolution in Western and Central Europe. Geological Society, London, *Memoirs* 32, 355–388. https://doi.org/10.1144/GSL.MEM.2006.032.01.22

Meier T., Soomro R.A., Viereck L., Lebedev S., Behrmann J.H., Weidle C., Cristiano L. & Hanemann R. 2016: Mesozoic and Cenozoic evolution of the Central European lithosphere. *Tectonophysics* 692, 58–73. https://doi.org/10.1016/j.tecto.2016.09.016

Mesa J. & Lange R.A. 2021: Origin of alkali olivine basalts and hawaiites in the western Mexican arc: Evidence of rapid phenocryst growth and magma mixing during ascent along fractures. *Geosphere* 17, 1–26. https://doi.org/10.1130/GES02365.1

Miller C. & Thöni M. 1997: Eo-Alpine eclogitisation of Permian MORB-type gabbros in the Koralpe (Eastern Alps, Austria): new geochronological, geochemical and petrological data. *Chemical Geology* 137, 283–310.

Miller C., Stosch H.-G. & Hoernes S. 1988: Geochemistry and origin of eclogites from the type locality Koralpe and Saualpe, Eastern Alps, Austria. *Chemical Geology* 67, 103–118.

Miller C., Zanetti A., Thöni M. & Konzett J. 2007: Eclogitisation of gabbroic rocks: Redistribution of trace elements and Zr in rutile thermometry in an Eo-Alpine subduction zone (Eastern Alps). *Chemical Geology* 239, 96–123. https://doi.org/10.1016/j.chemgeo.2007.01.001

Miller C., Thöni M., Goessler W. & Tessadri R. 2011: Origin and age of the Eisenkappel gabbro to granite suite (Carinthia, SE Austrian Alps). *Lithos* 125, 434–448. https://doi.org/10.1016/j.lithos.2011.03.003

Missoni S. & Gawlick H.-J. 2011: Evidence for Jurassic subduction from the Northern Calcareous Alps (Berchtesgaden; Austroalpine, Germany). *International Journal of Earth Sciences* 100, 1605–1631. https://doi.org/10.1007/s00531-010-0552-z

Mouthereau F., Angrand P., Jourdon A., Ternois S., Fillon C., Calassou S., Chevrot S., Ford M., Jolivet L., Manatschal G., Masini E., Thinon I., Vidal O. & Baudin. T. 2021: Cenozoic mountain building and topographic evolution in Western Europe: impact of billions of years of lithosphere evolution and plate kinematics. *BSGF – Earth Sciences Bulletin* 192, 56. https://doi.org/10.1051/bsgf/2021040

Neubauer F. 1988: The Variscan orogeny in the Austroalpine and Southalpine domains of the Eastern Alps. *Schweizerische Mineralogische und Petrographische Mitteilungen* 68, 339–349.

Neubauer F. & Genser J. 1990: Architektur und Kinematik der östlichen Zentralalpen – Eine Übersicht. *Mitteilungen des Naturwissenschaftlichen Vereins für Steiermark* 120, 203–219.

Neubauer F., Liu Y., Dong Y., Chang R., Genser J. & Yuan S. 2022: Pre-Alpine tectonic evolution of the Eastern Alps: From Protothetys to Paleotethys. *Earth-Science Reviews* 226, 103923. https://doi.org/10.1016/j.earscirev.2022.103923

Nievoll J. 1984: Der Südrand der Grauwackenzone zwischen Stübming und Neuberg (Obersteiermark, OK 103 Kindberg). *Mitteilungen der Österreichischen Geologischen Gesellschaft* 77, 63–71.

Nikishin A.M., Ziegler P.A, Abbott D., Brunet M.-F. & Cloetingh S. 2002: Permo–Triassic intraplate magmatism and rifting in Eurasia: implications for mantle plumes and mantle dynamics. *Tectonophysics* 351, 3–39. https://doi.org/10.1016/S0040-1951(02)00123-3

Oberhauser R. 1980: Der Geologische Aufbau Österreichs. *Springer*, Vienna, 1–699.

Oravecz É., Héja G. & Fodor L. 2023: Salt tectonics versus shortening: Recognizing pre-orogenic evaporite deformation in salt-bearing fold-and-thrust belts on the example of the Silica Nappe (Inner Western Carpathians). *Tectonics* 42, e2023TC007842. https://doi.org/10.1029/2023TC007842

Ortner H. & Sinah K. 2022: Thrust tectonics in the Wetterstein and Mieming mountains, and a new tectonic subdivision of the Northern Calcareous Alps of Western Austria and Southern Germany. International *Journal of Earth Sciences* 111, 543–571. https://doi.org/10.1007/s00531-021-02128-3

Pearce J.A. 1982: Trace element characteristics of lavas from destructive plate boundaries. In: Thorpe R.S. (Ed.): Andesites: Orogenic Andesites and Related Rocks. *John Wiley & Sons*, Chichester, 525–548.

Pearce J.A. 1983: Role of the sub-continental lithosphere in magma genesis at active continental margins. In: Hawkesworth C.J. & Norry M. J. (Eds.): Continental basalts and mantle xenoliths. *Shiva,* Orpington (London), and *Birkhauser,* Boston, Cambridge, Massachusetts, 230–249.

Pearce J.A.& Norry M.J. 1979: Petrogenetic Implications of Ti, Zr, Y, and Nb Variations in Volcanic Rocks. *Contributions to Mineralogy and Petrology* 69, 33–47. https://doi.org/10.1007/bf00375192

Petri B., Mohn G., Skrzypek E., Mateeva T., Galster F. & Manatschal G. 2017: U–Pb geochronology of the Sondalo gabbroic complex (Central Alps) and its position within the Permian post-Variscan extension. *International Journal of Earth Sciences* 106, 2873–2893. https://doi.org/10.1007/s00531-017-1465-x

Pfiffner A.O. 2014: Geology of the Alps. Second ed., *Wiley*, Chichester, 1–376.

Pilet S., Baker M.B., Muntener O. & Stolper A.M. 2011: Monte Carlo Simulations of Metasomatic Enrichment in the Lithosphere and Implications for the Source of Alkaline Basalts. *Journal of Petrology* 52, 1415–1442. https://doi.org/10.1093/petrology/egr007

Plašienka D. 2018: Continuity and Episodicity in the Early Alpine Tectonic Evolution of the Western Carpathians: How Large-Scale Processes Are Expressed by the Orogenic Architecture and Rock Record Data. *Tectonics* 37, 2029–2079. https://doi.org/10.1029/2017TC004779

Plöchinger et al. 1982: Geologische Karte von Österreich 1:50.000, Blatt 95 Sankt Wolfgang im Salzkammergut, mit Erläuterungen. *Geologische Bundesanstalt*, Vienna.

Putiš M., Soták J., Li Q.-L., Ondrejka M., Li X.-H., Hu Z., Ling X., Nemec O., Németh Z. & Ružička P. 2019: Origin and Age Determination of the Neotethys Meliata Basin Ophiolite Fragments in the Late Jurassic–Early Cretaceous Accretionary Wedge Mélange (Inner Western Carpathians, Slovakia). *Minerals* 9, 652. https://doi.org/10.3390/min9110652

Putiš M., Scherer E.E., Nemec O., Ondrejka M., Ackermann L. & Ružička P. 2023: Geochemistry, Lu–Hf garnet ages, and P–T conditions of blueschist from the Meliatic and Fatric nappes, Western Carpathians: Indicators of Neotethyan subduction. *Geosystems and Geoenvironment* 2, 100150. https://doi.org/10.1016/geogeo.2022.100150

Putiš M., Sláma J., Li Q.-L., Nemec O., Ondrejka M., Li X.-H., Koller F., Ackermann L., Strnad L. & Ružička P. 2024: Lithology, U–Pb zircon geochronology, and geochemistry of the Austroalpine Sieggraben Complex: Pre-Alpine vs. Alpine history. *Lithos* 482–483, 107739. https://doi.org/10.1016/j.lithos.2024.107739

Radvanec M., Konečný P., Ondrejka M., Putiš M., Uher P. & Németh Z. 2009: The Gemeric granites as an indicator of the crustal extension above the Late-Variscan subduction zone and during the early Alpine riftogenesis (Western Carpathians): an interpretation from the monazite and zircon ages dated by CHIME and SHRIMP methods. *Mineralia Slovaca* 41, 381–394.

Reiser M.K., Schuster R., Iglseder C., Gallhofer D. & Nievoll J. 2024: Geochronology, geochemistry, and geological evolution of the Troiseck-Floning and Rosskogel nappes (Eastern Alps): unraveling parallels between the Eastern Alps and Western Carpathians. *Swiss Journal of Geosciences* 117, 11. https://doi.org/10.1186/s00015-024-00456-5

Rowe M.C., Lassiter J.C. & Goff K. 2015: Basalt volatile fluctuations during continental rifting: An example from the Rio Grande Rift, USA. *Geochemistry, Geophysics, Geosystems* 16, 1254–1273. https://doi.org/10.1002/2014GC005649

Sassi R., Mazzoli C., Miller C. & Konzett J. 2004: Geochemistry and metamorphic evolution of the Pohorje Mountain eclogites from the easternmost Austroalpine basement of the Eastern Alps (Northern Slovenia). *Lithos* 78, 235–261. https://doi.org/10.1016/j.lithos.2004.05.002

Schmid S.M., Bernoulli D., Fügenschuh B., Matenco L., Schefer S., Schuster R., Tischler M. & Ustaszewski K. 2008: The Alpine–Carpathian–Dinaridic orogenic system: Correlation and evolution of tectonic units. *Swiss Journal of Geosciences* 101, 139–183. https://doi.org/10.1007/s00015-008-1247-3

Schmincke H.-U. 2012: Volcanism. *Springer*, Berlin, 1–324.

Schorn A., Neubauer F., Genser J. & Bernroider M. 2013: The Haselgebirge evaporitic mélange in central Northern Calcareous Alps (Austria): Part of the Permian to Lower Triassic rift of the Meliata ocean? *Tectonophysics* 583, 28–48. https://doi.org/10.1016/j.tecto.2012.10.016

Schulz B. 2017: Polymetamorphism in garnet micaschists of the Saualpe Eclogite Unit (Eastern Alps, Austria), resolved by automated SEM methods and EMP-Th-U-Pb monazite dating. *Journal of Metamorphic Geology* 35, 141–163. https://doi.org/10.1111/jmg.12224

Schuster R., Scharbert S., Abart R. & Frank W. 2001: Permo-Triassic extension and related HT/LP metamorphism in the Austroalpine–Southalpine realm. *Mitteilungen der Geologie- und Bergbaustudenten Österreichs* 44, 111–141.

Schuster R. & Stüwe K. 2008: Permian metamorphic event in the Alps. *Geology* 36, 603–606. https://doi.org/10.1130/G24703A.1

Sciunnach D. 2003: Fault-controlled stratigraphic architecture and magmatism in the western Orobic Basin (Lower Permian, Lombardy southern Alps). *Bollettino Società Geologica Italiana*, Volume Speciale 2, 49–58.

Slovenec D. & Šegvić B. 2024: The evolution of the Mesozoic lithosphere of northwestern Neotethys: a petrogenetic and geodynamic perspective: *Journal of the Geological Society* 181, jgs2023-132. https://doi.org/10.1144/jgs2023-132

Spahić D. 2024: Elusive Permian – Triassic Western Paleotethyan paleogeography: Towards the Early Cimmerian pre-Vardar configuration (Dinarides–Carpathian Balkan Belt). *Earth-Science Reviews* 256, 104857. https://doi.org/10.1016/j.earscirev.2024.104857

Spötl C. 1989: The Alpine Haselgebirge Formation, Northern Calcareous Alps (Austria): Permo-Scythian evaporites in an alpine thrust system. *Sedimentary Geology* 65, 113–125. https://doi.org/10.1016/0037-0738(89)90009-2

Stampfli G.M. 1996: The intra-Alpine terrain: A Paleotethyan remnant in the Alpine Variscides. *Eclogae Geologicae Helvetiae* 89, 13–42.

Stampfli G.M. & Mosar J. 1999: The making and becoming of Apulia. *Memorie di Scienze Geologiche* 51, 141–154.

Stampfli G.M., Hochard C., Vérard C., Wilhem C. & von Raumer J. 2013: The formation of Pangea. *Tectonophysics* 593, 1–19. https://doi.org/10.1016/j.tecto.2013.02.037

Strauss P., Granado P. & Muñoz J. 2021: Subsidence analysis of salt tectonics-driven carbonate minibasins (Northern Calcareous Alps, Austria). *Basin Research* 33, 968–990. https://doi.org/10.1111/bre.12500

Strauss P., Granado P., Muñoz J.A., Böhm K. & Schuster R. 2023: The Northern Calcareous Alps revisited: Formation of a hyperextended margin and mantle exhumation in the Northern Calcareous Alps sector of the Neo-Tethys (Eastern Alps, Austria). *Earth Science Reviews* 243, 104488. https://doi.org/10.1016/j.earscirev.2023.104488

Summesberger H. 1991: Geologische Karte von Österreich 1:50.000, Blatt 75 Puchberg am Schneeberg 1:50.000. *Geologische Bundesanstalt*, Vienna.

Sun S.-S. 1982: Chemical composition and origin of the Earth's primitive mantle. *Geochimica et Cosmochimica Acta* 46, 179–192.

Thöni M. 2006: Dating eclogite-facies metamorphism in the eastern Alps – Approaches, results, interpretations: A review. *Mineralogy and Petrology* 88, 123–148. https://doi.org/10.1007/s00710-006-0153-5

Thöni M. & Jagoutz E. 1993: Isotopic constraints for eo-Alpine high-P metamorphism in the Austroalpine nappes of the eastern Alps: Bearing on Alpine orogenesis. *Schweizerische Mineralogische und Petrographische Mitteilungen* 73, 177–189.

Tollmann A. 1963: Ostalpensynthese. *Deuticke*, Vienna, 1–256.

Tollmann A. 1972: Alter und Stellung des Alpinen Verrucano in den Ostalpen. *Verhandlungen der Geologischen Bundesanstalt* 1972, 83–95.

Tollmann A. 1985: Geologie von Österreich. Außerzentralalpiner Anteil, *Deuticke*, Vienna, 1–710.

Tortelli G., Gioncada A., Pagli C., Braschi E., Gebru E.F. & Keir D. 2022: Constraints on the magma source and rift evolution from geochemistry of the Stratoid flood basalts (Afar, Ethiopia). *Geochemistry, Geophysics, Geosystems* 23, e2022GC010434. https://doi. org/10.1029/2022GC010434

van Hinsbergen D.J.J., Torsvik T.H., Schmid S.M., Maţenco L.C., Maffione M., Vissers R.L.M., Gürer D & Spakman W 2020: Orogenic architecture of the Mediterranean region and kinematic reconstruction of its tectonic evolution since the Triassic. *Gondwana Research* 81, 79–229. https://doi.org/10.1016/j.gr.2019.07.009

Veselá P. & Lammerer B. 2008: The Pfitsch-Mörchner Basin, an example of the post-Variscan sedimentary evolution in the Tauern Window (eastern Alps). *Swiss Journal of Geosciences* 101, 73–88. https://doi.org/10.1007/s00015-008-1293-x

Veselá P., Lammerer B., Wetzel A., Söllner F. & Gerdes A. 2008: Post-Variscan to Early Alpine sedimentary basins in the Tauern Window (eastern Alps). In: Siegesmund S., Fügenschuh B. & Froitzheim M. (Eds.): Tectonic Aspects of the Alpine–Dinaride–Carpathian System. *Geological Society, London, Special Publication* 298, 83–100. https://doi.org/10.1144/SP298.5

Villaseñor G., Catlos E.J., Broska I., Kohút M., Hraško Ľ., Aguilera K., Etzel T.M., Kyle R.J. & Stockli D.F. 2021: Evidence for widespread mid-Permian magmatic activity related to rifting following the Variscan orogeny (Western Carpathians). *Lithos* 390–391, 106083. https://doi.org/10.1016/j.lithos.2021.106083

von Hauer F. 1879: Melaphyr vom Hallstätter Salzberge. *Verhandlungen der Geologischen Reichsanstalt* 1879, 252–254.

von Quadt A., Haunschmid B. & Finger F. 1999: Mid-Permian A-type plutonism in the eastern Tauern-Window. *European Journal of Mineralogy* 11, Beiheft 1, 185.

Vozárová A., Vozár J. & Mayr M. 1999: High-pressure metamorphism of basalts in the evaporite sequence of the Haselgebirge: An evidence from Bad Ischl (Austria). *Abhandlungen der Geologischen Bundesanstalt* 56, 325–330.

White J.C., Neave D.A., Rotolo S.G. & Parker D.F. 2020: Geochemical constraints on basalt petrogenesis in the Strait of Sicily Rift Zone (Italy): Insights into the importance of short length-scale mantle heterogeneity. *Chemical Geology* 545, 119650. https://doi.org/10.1016/j.chemgeo.2020.119650

Willcock M.A.W., Cas R.A.F., Giordano G. & Morelli C. 2013: The eruption, pyroclastic flow behaviour, and caldera in-filling processes of the extremely large volume (>1290 km³), intra- to extra-caldera, Permian Ora (Ignimbrite) Formation, Southern Alps, Italy. *Journal of Volcanology and Geothermal Research* 265, 102–126. https://doi.org/10.1016/j.jvolgeores.2013.08.012

Wilson M. 1989: Igneous Petrogenesis A Global Tectonic Approach. *Springer*, London, 1–466

Winchester J.A. & Floyd P.A. 1977: Geochemical discrimination of different magma series and their differentiation products using immobile elements. *Chemical Geology* 20, 325–343. https://doi.org/10.1016/0009-2541(77)90057-2

Xia L. & Li X. 2019: Basalt geochemistry as a diagnostic indicator of tectonic setting. *Gondwana Research* 65, 43–67. https://doi.org/10.1016/j.gr.2018.08.006

Xu R., Liu Y., Wang X.C., Foley S.F., Zhang Y. & Yuan H. 2020: Generation of continental intraplate alkali basalts and implications for deep carbon cycle. *Earth-Science Reviews* 201, 103073. https://doi.org/10.1016/j.earscirev.2019.103073

Yu Y., Zong K., Yuan Y., Klemd R., Wang X.-S., Guo J., Xu R., Hu Z. & Liu Y. 2022: Crustal Contamination of the Mantle-Derived Liuyuan Basalts: Implications for the Permian Evolution of the Southern Central Asian Orogenic Belt. *Journal of Earth Science* 33, 1081–1094. https://doi.org/10.1007/s12583-022-1706-1

Yuan S., Neubauer F., Liu Y., Genser J., Liu B., Yu S., Chang R. & Guan Q. 2020: Widespread Permian granite magmatism in Lower Austroalpine units: significance for Permian rifting in the Eastern Alps. *Swiss Journal of Geosciences* 113, 18. https://doi.org/10.1186/s00015-020-00371-5

Ziegler P.A. 1990: Geological Atlas of Western and Central Europe. Shell International Petroleum Mij. B.V. Second ed., distributed by Geological Society, *Publishing House*, Bath, London, 1–239.

Ziegler P.A. 1993: Late Palaeozoic–Early Mesozoic Plate Reorganization: Evolution and Demise of the Variscan Fold Belt. In: Raumer J.v. & Neubauer F. (Eds.): Pre-Mesozoic Geology in the Alps. *Springer*, Berlin, 203–216.

Ziegler P.A. & Dèzes P. 2006: Crustal Evolution of Western and Central Europe. In: Gee D.G. & Stephenson R.A. (Eds.): European Lithosphere Dynamics. *Geological Society London Memoirs* 32, 43–56. https://doi.org/10.1144/GSL.MEM.2006.032.01.03

Zirkl E.J. 1957: Der Melaphyr von Hallstatt. *Jahrbuch der Geologischen Bundesanstalt* 100, 137–177.